

Vibration analysis of porous FGM plate resting on elastic foundations: Effect of the distribution shape of porosity

Bekki Hadj^{1,2}, Benferhat Rabia^{1,2} and Tahar Hassaine Daouadji^{*1,2}

¹Laboratory of Geomatics and sustainable development, University of Tiaret, Algeria

²Department of Civil Engineering, Ibn Khaldoun University of Tiaret, Algeria

(Received August 6, 2020, Revised December 3, 2020, Accepted January 17, 2021)

Abstract. The porosity of functionally graded materials (FGM) can affect the static and dynamic behavior of plates, which is important to take this aspect into account when analyzing such structures. The present work aims to study the effect of the distribution shape of porosity on the free vibration response of simply supported FG plate reposed on the Winkler-Pasternak foundation. A refined theory of shear deformation is expanded to study the influence of the distribution shape of porosity on the free vibration behavior of FG plates. The findings showed that the distribution shape of porosity significantly influences the free vibration behavior of thick rectangular FG plates for small values of Winkler-Pasternak elastic foundation parameters.

Keywords: FGM plate; higher-order theory; free vibration behavior; volume fraction of porosity; Winkler-Pasternak elastic foundation

1. Introduction

Functionally graded materials (FGMs) are considered as novel composite materials that are generally used in aerospace, nuclear, automotive, civil, marine technology, and defense industries. FGMs are, macroscopically, non-homogeneous compounds, in which the material properties vary continuously from one interface to the other. The continuity of the material properties reduces the influence of the presence of interfaces and avoids high interfacial stresses. The first applications of FGMs are in high-temperature environments, but their applications are continuously expanding, which requires a better knowledge of their mechanical behavior. Thus, several research works have been undertaken to study the static as well as the dynamic behavior of FGM plates. Such structures are usually supported by elastic foundations (Chaabane *et al.* 2019, Berghouti *et al.* 2019, Hassaine Daouadji *et al.* 2020). The most foundation models used to describe the mechanical behavior of foundations are the Pasternak model containing two parameters and the Winkler model which is a special case of the first one. In fact, the Winkler model assimilates the foundation as a series of separated vertical springs without coupling effects between each other, while the Pasternak model takes into account the interactions between springs and overcomes the problem of discontinuous deflection on the interacted surface of the plate.

Based on the First-order shear deformation theory (FSDT), several works have been carried out

*Corresponding author, Professor, E-mail: daouadjitahar@gmail.com

to study the bending of functionally graded plates. Among others, we can cite the work of several researchers, namely: Praveen and Reddy 1998, Refrafi, *et al.* 2020, Tounsi *et al.* 2020, Hassaine Daouadji *et al.* 2016, Zohra *et al.* 2016, Kaddari *et al.* 2020, Benhenni *et al.* 2019, Rabia *et al.* 2018, Al-Furjan *et al.* 2020c, Al-Furjan *et al.* 2020d, Al-Furjan *et al.* 2021, Alimirzaei *et al.* 2019, Bensattalah *et al.* 2018, Daouadji *et al.* 2016b, Hamrat *et al.* 2020, Hassaine Daouadji 2013, Balubaid *et al.* 2019, Batou *et al.* 2019, Belbachir *et al.* 2019, Bellal *et al.* 2020, Bourada *et al.* 2020 and Bekki *et al.* 2019). In addition, the refined theory of shear deformation has proven its performance compared to other theories because it contains limited unknown variables (only 4 parameters) (Draiche *et al.* 2019, Belbachir *et al.* 2020, Thai *et al.* 2013, Khiloun *et al.* 2020, Matouk *et al.* 2020, Mahmoudi *et al.* 2019, Bensattalah *et al.* 2016, Bouakaz *et al.* 2014, Chaded *et al.* 2018, Chergui *et al.* 2019, Daouadji *et al.* 2016a, Rabhi *et al.* 2020, Rahmani *et al.* 2020, Zine *et al.* 2020, Hassaine Daouadji *et al.* 2016, Mohamed Amine *et al.* 2019, Rabahi *et al.* 2019, Rabia *et al.* 2016, Bourada *et al.* 2020 and Chaabane *et al.* 2019), which makes its use very practical. Some researchers were particularly interested in studying the free vibration response of functionally graded plates. Talha *et al.* (2010) studied the free vibration and static analysis of functionally graded material (FGM) plates using higher-order shear deformation theory (HSDT) by modifying the transverse displacement by conjunction with finite element models. An exact three-dimensional elastic model was proposed by Ait Atmane *et al.* (2019) to study the free vibration response of functionally graded one-layered and sandwich simply-supported plates and shells. An interesting study based on the FSDT theory was presented by several researchers (Zhao *et al.* 2009, Boulefrakh *et al.* 2019, Boussoula *et al.* 2020, Chikr *et al.* 2020, Hussain *et al.* 2020, Khadimallah *et al.* 2020, Al-Furjan *et al.* 2020a, Abdederak *et al.* 2018, Abdelhak *et al.* 2016, Adim B *et al.* 2018, Benferhat *et al.* 2019, Belkacem *et al.* 2016, Benhenni *et al.* 2018, Rabahi *et al.* 2020, Tounsi *et al.* 2008, Tahar *et al.* 2016, Bensattalah *et al.* 2020, Al-Furjan *et al.* 2020b, Hassaine Daouadji 2017, Matsunaga *et al.* 2008 and Hosseini-Hashemi *et al.* 2011) and focused on the analysis of rectangular FG plates with different boundary conditions. On the other hand, the functionally graded materials (FGM) used in plates may be imperfects that are due to a possible porosity volume fraction in them, which can altercate their mechanical behavior. Benferhat *et al.* (2016) studied the effect of porosity on the bending and free vibration response of functionally graded plates resting on Winkler-Pasternak foundations by introducing in the mathematical formulation a volume fraction of porosity (α). But the distribution shape of porosity can also affect both static and dynamic behavior of FG plates; such influence has been highlighted very recently by Bekki *et al.* (2019) who studied the influence of several forms of porosity on the bending FG plates resting on elastic foundations.

The present work is aimed to study the effect of the distribution shape of porosity on the free vibration response of simply supported FGM plates resting on elastic foundation. The imperfection or porosity is included using a modified mixture law covering the porosity phases as proposed by Wattanasakulponga *et al.* (2014). The equation of motion for FGM plates is obtained through the minimum total potential energy and the principle of Hamilton. The effects of pore volume fraction, geometry ratio, and thickness ratio on the free vibration response of FGM plate are also investigated.

2. Mathematical formulation

2.1 Geometric configuration

In this study, we consider a FGM plate of length a , width b and total thickness h , made of mixture

of metal and ceramics, in which the composition is varied from the top to the bottom surface. The material in top surface and in bottom surface is ceramic and metal respectively (Fig.1).

We also consider an imperfect FGM plate with a volume fraction of porosity α ($\alpha \ll 1$), uniformly distributed between the metal and the ceramic. We use the modified mixture rule proposed by Wattanasakulpong and Ungbhakorn (2014) as

$$P = P_m \left(V_m - \frac{\alpha}{2} \right) + P_c \left(V_c - \frac{\alpha}{2} \right) \quad (1)$$

Now, the total volume fraction of the metal and ceramic is: $V_m + V_c = 1$ and the power law of volume fraction of the ceramic is described as

$$V_c = \left(\frac{z}{h} + \frac{1}{2} \right)^p \quad (2a)$$

The modified mixture rule becomes

$$P = (P_c - P_m) \left(\frac{z}{h} + \frac{1}{2} \right)^p + P_m - (P_c + P_m) \frac{\alpha}{2} \quad (2b)$$

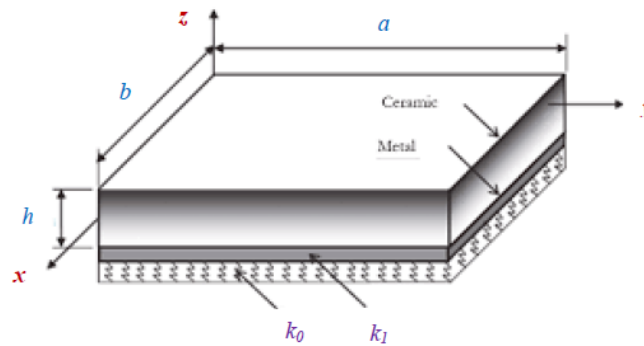


Fig. 1 Geometry and dimensions of the FGM plate resting on elastic foundation

Where, k is the power law index that takes values greater than or equals to zero. The FGM plate becomes a fully ceramic plate when k is set to zero and fully metal for large value of “ p ”.

The Young’s modulus (E) of the imperfect FG can be written as a functions of thickness coordinate, z (middle surface), as follows (Benferhat *et al.* 2016, Hassaine Daouadji *et al.* 2019, Rabahi *et al.* 2016)

$$E(z) = (E_c - E_m) \left(\frac{z}{h} + \frac{1}{2} \right)^p + E_m - (E_c + E_m) \frac{\alpha}{2} \quad (3)$$

2.2 Material properties

The material properties of a perfect FGM plate can be obtained when the volume fraction of porosity α is set to zero. Considering that the Poisson ratio ν varies slightly, it can be assumed to be constant and fixed at $\nu=0.3$. The properties of the material of the FGM plate are supposed to vary according to a power law distribution of the volume fraction of the constituents. The properties of the materials used in this analysis are presented in Table 1.

Table 1 Material proprieties

Materiel	Properties	
	E (GPa)	ν
Ceramic (Alumina, Al_2O_3)	380	0.3
Metal (Aluminum Al)	70	0.3

Table 2 Deferent distribution forms of porosity

Distribution forms of Porosity		Elastic Modulus Expression	
Uniformly distributed	UD	$E = (e_c - e_m)\left(\frac{z}{h} + \frac{1}{2}\right)^p + e_m - (e_c + e_m)\frac{\alpha}{2}$	(4a)
Linear functionally graded	O- L	$E = (e_c - e_m)\left(\frac{z}{h} + \frac{1}{2}\right)^p + e_m - (e_c + e_m)\frac{\alpha}{2}\left(1 - 2\frac{ z }{h}\right)$	(4b)
	X- L	$E = (e_c - e_m)\left(\frac{z}{h} + \frac{1}{2}\right)^p + e_m - (e_c + e_m)\frac{\alpha}{2}\left(2\frac{z}{h}\right)$	(4c)
	V- L	$E = (e_c - e_m)\left(\frac{z}{h} + \frac{1}{2}\right)^p + e_m - (e_c + e_m)\frac{\alpha}{2}\left(\frac{1}{2} + \frac{z}{h}\right)$	(4d)
	Λ - L	$E = (e_c - e_m)\left(\frac{z}{h} + \frac{1}{2}\right)^p + e_m - (e_c + e_m)\frac{\alpha}{2}\left(\frac{1}{2} - \frac{z}{h}\right)$	(4e)
Non-Linear functionally graded	O- NL	$E = (e_c - e_m)\left(\frac{z}{h} + \frac{1}{2}\right)^p + e_m - (e_c + e_m)\frac{\alpha}{2}\left(1 - 2\frac{ z }{h}\right)^2$	(4f)
	X- NL	$E = (e_c - e_m)\left(\frac{z}{h} + \frac{1}{2}\right)^p + e_m - (e_c + e_m)\frac{\alpha}{2}\left(2\frac{z}{h}\right)^2$	(4g)
	V- NL	$E = (e_c - e_m)\left(\frac{z}{h} + \frac{1}{2}\right)^p + e_m - (e_c + e_m)\frac{\alpha}{2}\left(\frac{1}{2} + \frac{z}{h}\right)^2$	(4h)
	Λ - NL	$E = (e_c - e_m)\left(\frac{z}{h} + \frac{1}{2}\right)^p + e_m - (e_c + e_m)\frac{\alpha}{2}\left(\frac{1}{2} - \frac{z}{h}\right)^2$	(4i)

Several forms of porosity have been studied in the present work, such as “O”, “X”, “V” and “ Λ ” forms with linear and non-linear expressions (Table 2).

2.3 Displacement field and strains

Based on of the theory of the higher order shear deformation plate, displacement elements are assumed as follow

$$\begin{aligned}
 u(x, y, z) &= u_0(x, y) - z \frac{\partial w_b}{\partial x} - z \left[1 + \frac{3\pi}{2} \operatorname{sech}^2\left(\frac{1}{2}\right) \right] - \frac{3\pi}{2} h \tanh\left(\frac{z}{h}\right) \frac{\partial w_s}{\partial x} \\
 v(x, y, z) &= v_0(x, y) - z \frac{\partial w_b}{\partial y} - z \left[1 + \frac{3\pi}{2} \operatorname{sech}^2\left(\frac{1}{2}\right) \right] - \frac{3\pi}{2} h \tanh\left(\frac{z}{h}\right) \frac{\partial w_s}{\partial y} \\
 w(x, y, z) &= w_b(x, y) + w_s(x, y)
 \end{aligned} \tag{5}$$

Linear deformation can be obtained from kinematic relationships as

$$\begin{aligned}
 \epsilon_x &= \epsilon_x^0 + z k_x^b + z \left[1 + \frac{3\pi}{2} \operatorname{sech}^2\left(\frac{1}{2}\right) \right] - \frac{3\pi}{2} h \tanh\left(\frac{z}{h}\right) k_x^s \\
 \epsilon_y &= \epsilon_y^0 + z k_y^b + z \left[1 + \frac{3\pi}{2} \operatorname{sech}^2\left(\frac{1}{2}\right) \right] - \frac{3\pi}{2} h \tanh\left(\frac{z}{h}\right) k_y^s \\
 \gamma_{xy} &= \gamma_{xy}^0 + z k_{xy}^b + z \left[1 + \frac{3\pi}{2} \operatorname{sech}^2\left(\frac{1}{2}\right) \right] - \frac{3\pi}{2} h \tanh\left(\frac{z}{h}\right) k_{xy}^s \\
 \gamma_{yz} &= 1 - \frac{d\left(z\left[1 + \frac{3\pi}{2} \operatorname{sech}^2\left(\frac{1}{2}\right)\right] - \frac{3\pi}{2} h \tanh\left(\frac{z}{h}\right)\right)}{dz} \gamma_{yz}^s \\
 \gamma_{xz} &= 1 - \frac{d\left(z\left[1 + \frac{3\pi}{2} \operatorname{sech}^2\left(\frac{1}{2}\right)\right] - \frac{3\pi}{2} h \tanh\left(\frac{z}{h}\right)\right)}{dz} \gamma_{xz}^s \\
 \epsilon_z &= 0
 \end{aligned} \tag{6}$$

Where

$$\begin{aligned}
 \epsilon_x^0 &= \frac{\partial u_0}{\partial x}, \quad k_x^b = -\frac{\partial^2 w_b}{\partial x^2}, \quad k_x^s = -\frac{\partial^2 w_s}{\partial x^2} \\
 \epsilon_y^0 &= \frac{\partial v_0}{\partial y}, \quad k_y^b = -\frac{\partial^2 w_b}{\partial y^2}, \quad k_y^s = -\frac{\partial^2 w_s}{\partial y^2} \\
 \gamma_{xy}^0 &= \frac{\partial u_0}{\partial x} + \frac{\partial v_0}{\partial y}, \quad k_{xy}^b = -2\frac{\partial^2 w_b}{\partial x \partial y}, \quad k_{xy}^s = -2\frac{\partial^2 w_s}{\partial x \partial y} \\
 \gamma_{yz}^s &= \frac{\partial w_s}{\partial y}, \quad \gamma_{xz}^s = \frac{\partial w_s}{\partial x}, \quad g(z) = 1 - \frac{f(z)}{dz} \\
 f(z) &= z \left[1 + \frac{3\pi}{2} \operatorname{sech}^2\left(\frac{z}{2}\right) \right] - \frac{3\pi}{2} h \tanh\left(\frac{z}{h}\right)
 \end{aligned} \tag{7}$$

The linear constitutive relationships of a FG plate can be written as

$$\begin{Bmatrix} \sigma_x \\ \sigma_y \\ \tau_{xy} \end{Bmatrix} = \begin{bmatrix} \frac{E(z)}{1-\nu^2} & \frac{\nu E(z)}{1-\nu^2} & 0 \\ \frac{\nu E(z)}{1-\nu^2} & \frac{E(z)}{1-\nu^2} & 0 \\ 0 & 0 & \frac{E(z)}{2(1+\nu)} \end{bmatrix} \begin{Bmatrix} \epsilon_x \\ \epsilon_y \\ \gamma_{xy} \end{Bmatrix} \tag{8}$$

$$\begin{Bmatrix} \tau_{yz} \\ \tau_{zx} \end{Bmatrix} = \begin{bmatrix} \frac{E(z)}{2(1+\nu)} & 0 \\ 0 & \frac{E(z)}{2(1+\nu)} \end{bmatrix} \begin{Bmatrix} \gamma_{yz} \\ \gamma_{zx} \end{Bmatrix} \tag{9}$$

2.4 Equilibrium equations

To obtain the equations of motion, the energy method is adopted and the total energy of structure is needed.

$$U = \frac{1}{2} \int_V \sigma_{ij} \epsilon_{ij} dV = \frac{1}{2} \int_V (\sigma_x \epsilon_x + \sigma_y \epsilon_y + \sigma_{xy} \gamma_{xy} + \sigma_{yz} \gamma_{yz} + \sigma_{xz} \gamma_{xz}) dV \tag{10}$$

Also, using the Hamilton's principle, the governing equations of motion can be obtained as the equilibrium equations that govern can be derived using the principle of virtual displacements as

$$\delta \int_{t_1}^{t_2} (U + U_F - K - W) dt = 0 \tag{11}$$

Where U is the strain energy and K is the kinetic energy of the FG plate, U_F is the strain energy of foundation and W is the work of external forces. Employing the minimum of the total energy principle leads to a general equation of motion and boundary conditions. Taking the variation of the above equation and integrating by parts

$$\begin{aligned}
 \int_{t_1}^{t_2} \left[\int_V [\sigma_x \delta \epsilon_x + \sigma_y \delta \epsilon_y + \tau_{xy} \delta \gamma_{xy} + \tau_{yz} \delta \gamma_{yz} + \tau_{zx} \delta \gamma_{zx} - \rho(\ddot{u} \delta u + \ddot{v} \delta v + \ddot{w} \delta w)] dv \right. \\
 \left. + \int_A [f_e \delta w] dA \right] dt
 \end{aligned} \tag{12}$$

The integral represents the second derivative with respect to time and f_e is the density of the foundation reaction force. For the Pasternak foundation model, f_e can written as

$$f_e = k_0 w - k_1 \nabla^2 w \quad (13)$$

K_0 and K_1 are the transverse and shear stiffness coefficients of the foundation respectively. The stress resultants are given as

$$\begin{Bmatrix} N \\ M^b \\ M^s \end{Bmatrix} = \begin{bmatrix} A & B & B^s \\ B & D & D^s \\ B^s & D^s & H^s \end{bmatrix} \begin{Bmatrix} \varepsilon \\ k^b \\ k^s \end{Bmatrix}; S = A^s \gamma \quad (14)$$

Wher

$$N = \{N_x, N_y, N_{xy}\}^t, \quad M^b = \{M_x^b, M_y^b, M_{xy}^b\}^t \quad (15a)$$

$$M^s = \{M_x^s, M_y^s, M_{xy}^s\}^t, \quad \varepsilon = \{\varepsilon_x^0 + \varepsilon_y^0 + \varepsilon_{xy}^0\}^t \quad (15b)$$

$$k^b = \{k_x^b, k_y^b, k_{xy}^b\}^t, \quad k^s = \{k_x^s, k_y^s, k_{xy}^s\}^t \quad (15c)$$

$$A = \begin{bmatrix} A_{11} & A_{12} & 0 \\ A_{12} & A_{22} & 0 \\ 0 & 0 & A_{66} \end{bmatrix}, \quad B = \begin{bmatrix} B_{11} & B_{12} & 0 \\ B_{12} & B_{22} & 0 \\ 0 & 0 & A_{66} \end{bmatrix}, \quad D = \begin{bmatrix} D_{11} & D_{12} & 0 \\ D_{12} & D_{22} & 0 \\ 0 & 0 & D_{66} \end{bmatrix} \quad (15d)$$

$$B^s = \begin{bmatrix} B_{11}^s & B_{12}^s & 0 \\ B_{12}^s & B_{22}^s & 0 \\ 0 & 0 & B_{66}^s \end{bmatrix}, \quad D^s = \begin{bmatrix} D_{11}^s & D_{12}^s & 0 \\ D_{12}^s & D_{22}^s & 0 \\ 0 & 0 & D_{66}^s \end{bmatrix}, \quad H^s = \begin{bmatrix} H_{11}^s & H_{12}^s & 0 \\ H_{12}^s & H_{22}^s & 0 \\ 0 & 0 & H_{66}^s \end{bmatrix} \quad (15e)$$

$$S = \{S_{xz}^s, S_{yz}^s\}^t, \quad \gamma = \{\gamma_{xz}, \gamma_{yz}\}^t, \quad A^s = \begin{bmatrix} A_{44}^s & 0 \\ 0 & A_{55}^s \end{bmatrix} \quad (15f)$$

Stiffness components and inertias are given as

$$\{A_{ij}, B_{ij}, C_{ij}, D_{ij}, E_{ij}, G_{ij}\} = \int_{-h/2}^{h/2} \{1, z, f(z), z^2, zf(z), [f(z)]^2\} Q_{ij} dz \quad (16)$$

Following the Navier solution procedure, we assume that the following solution form u_0 , v_0 , w_b and w_s , satisfies the boundary conditions of rectangular FG plate simply supported

$$\begin{Bmatrix} u_0 \\ v_0 \\ w_b \\ w_s \end{Bmatrix} = \sum_{m=1}^{\infty} \sum_{n=1}^{\infty} \begin{Bmatrix} U_{mn} \cos(\lambda x) \sin(\mu y) e^{i\omega t} \\ V_{mn} \sin(\lambda x) \cos(\mu y) e^{i\omega t} \\ W_{bmn} \sin(\lambda x) \sin(\mu y) e^{i\omega t} \\ W_{smn} \sin(\lambda x) \sin(\mu y) e^{i\omega t} \end{Bmatrix} \quad (17)$$

Where: $\lambda = m\pi/a$, $\mu = n\pi/b$ and U_{mn} , V_{mn} , W_{bmn} , W_{smn} being arbitrary parameters and ω denotes the Eigen frequency associated with (m,n)th Eigen mode. One obtains the following operator equation

$$([K] - \omega^2 [M])\{\Delta\} = \{0\} \quad (18)$$

Where: $\{\Delta\} = \{U, V, W_b, W_s\}^t$ and $[K]$ and $[M]$, stiffness and mass matrices, respectively, and represented as

$$[K] = \begin{bmatrix} a_{11} & a_{12} & a_{13} & a_{14} \\ a_{12} & a_{22} & a_{23} & a_{24} \\ a_{13} & a_{23} & a_{33} & a_{34} \\ a_{14} & a_{24} & a_{34} & a_{44} \end{bmatrix} \quad (19a)$$

$$[M] = \begin{bmatrix} m_{11} & 0 & 0 & 0 \\ 0 & m_{22} & 0 & 0 \\ 0 & 0 & m_{33} & m_{34} \\ 0 & 0 & m_{34} & m_{44} \end{bmatrix} \quad (19b)$$

In which

$$a_{11} = A_{11}\alpha^2 + A_{66}\beta^2 \quad (20a)$$

$$a_{12} = \alpha\beta(A_{12} + A_{66}) \quad (20b)$$

$$a_{13} = -B_{11}\alpha^3 \quad (20c)$$

$$a_{14} = C_{11}\alpha^2 + C_{66}\beta^2 \quad (20d)$$

$$a_{15} = \alpha\beta(C_{12} + C_{66}) \quad (20e)$$

$$a_{22} = A_{66}\alpha^2 + A_{22}\beta^2 \quad (20f)$$

$$a_{23} = -B_{22}\beta^2 \quad (20g)$$

$$a_{24} = \alpha\beta(C_{12} + C_{66}) \quad (20h)$$

$$a_{25} = C_{66}\alpha^2 + C_{66}\beta^2 \quad (20i)$$

$$a_{33} = D_{11}\alpha^4 + 2D_{12}\alpha^2\beta^2 + 4D_{66}\alpha^2\beta^2 + D_{22}\beta^4 + k_0 + k_1(\alpha^2 + \beta^2) \quad (20j)$$

$$a_{34} = -E_{11}\alpha^3 - E_{12}\alpha\beta^2 - 2E_{66}\alpha\beta^2 \quad (20k)$$

$$a_{35} = -E_{12}\alpha^2\beta - 2E_{66}\alpha^2\beta - E_{22}\beta^3 \quad (20l)$$

$$a_{44} = F_{55} + G_{11}\alpha^2 + G_{66}\beta^2 \quad (20m)$$

$$a_{45} = \alpha\beta(G_{12} + G_{66}) \quad (20n)$$

$$a_{55} = F_{44} + G_{66}\alpha^2 + G_{22}\beta^2 \quad (20o)$$

$$\text{And: } \alpha = m\pi/a, \beta = n\pi/b \quad (21)$$

The natural frequencies of FG plate can be found from the nontrivial solution of Eq. (18).

3. Results and discussion:

In the present study, the effect of the distribution shape of porosity on the normalized Eigen frequency parameter is investigated for rectangular FG plates resting on Winkler-Pasternak elastic foundations.

In order to verify the accuracy of the present solution, some illustrative examples whose results are compared with the solutions available in the literature.

The Fundamental frequency parameters in the form of $\bar{\omega} = \omega h \sqrt{\rho_c/E_c}$ of the SSSS square FG plates ($a/b=1$) for different values of the thickness to length ratios ($h/a=0.05, 0.1, \text{ and } 0.2$) are presented in Table 3, for a gradient index $P=0, 1, 4$ and 10 . The plates are made of a mixture of aluminum (Al) and alumina (Al_2O_3). The calculated fundamental frequency parameters are compared with those reported in literature (Tounsi *et al.* 2020, Ait Atmane *et al.* 2019, Kaci *et al.* 2020, Refrafi *et al.* 2020).

As we can see on Table 3, close agreements were obtained between the results of the present method and those of literature, with precision up to 2 to 3 digits after the decimal point. However;

Table 3 Comparison of fundamental frequency parameters $\bar{\omega} = \omega h \sqrt{\rho_c/E_c}$ for SSSS Al/Al₂O₃ square plates ($a/b=1$)

Thickness-to-length ratio h/a	Method	Gradient index P				
		0	1	4	10	
0.05	Tounsi <i>et al.</i> (2020) (FSDT)	0.01480	0.01150	0.01013	0.00963	
	Ait Atmane <i>et al.</i> (2019) (FSDT)	0.01464	0.01118	0.00970	0.00931	
	Present	$\alpha=0$	0.014799	0.011307	0.009805	0.009408
		$\alpha=0.1$	0.015470	0.011911	0.010378	0.009966
		$\alpha=0.2$	0.016240	0.012623	0.011055	0.010590
0.1	Tounsi <i>et al.</i> (2020) (FSDT)	0.05769	0.04454	0.03825	0.03627	
	Kaci <i>et al</i> (2020) (2D)	0.05777	0.04427	0.03811	0.03642	
	Refrafi <i>et al</i> (2020) (FSDT)	0.06382	0.04889	0.04230	0.04047	
	Ait Atmane <i>et al.</i> (2019) (FSDT)	0.05673	0.04346	0.03757	0.03591	
	Present	$\alpha=0$	0.057697	0.044175	0.038047	0.036365
		$\alpha=0.1$	0.060236	0.046452	0.040041	0.038119
		$\alpha=0.2$	0.063152	0.049122	0.042237	0.039529
0.2	Tounsi <i>et al.</i> (2020) (FSDT)	0.2112	0.1650	0.1371	0.1304	
	Kaci <i>et al</i> (2020) (2D)	0.2121	0.1640	0.1383	0.1306	
	Refrafi <i>et al</i> (2020) (FSDT)	0.2334	0.1802	0.1543	0.1462	
	Ait Atmane <i>et al.</i> (2019) (FSDT)	0.2055	0.1587	0.1356	0.1284	
	Present	$\alpha=0$	0.21129	0.16288	0.137513	0.129954
		$\alpha=0.1$	0.219792	0.170345	0.142363	0.132317
		$\alpha=0.2$	0.229497	0.178942	0.146257	0.129287

Table 4 Comparison of fundamental frequency parameters $\tilde{\beta} = \omega a^2 \sqrt{\rho_c/E_c}/h$ for SSSS Al/Al₂O₃ square plates ($a/b=1$)

Thickness-to-length ratio h/a	Method	Gradient index P				
		0	1	5	10	
0.1	Tounsi <i>et al.</i> (2020) (FSDT)	5.7693	4.4545	3.7837	3.6277	
	Ait Atmane <i>et al.</i> (2019) (FSDT)	5.6763	4.3474	3.7218	3.5923	
	Present	$\alpha=0$	5.76966	4.41750	3.76613	3.63654
		$\alpha=0.1$	6.02364	4.64520	3.95917	3.81187
		$\alpha=0.2$	6.31516	4.91219	4.16100	3.95287

a certain difference of around 3% is recorded by comparing the results with those of Ait Atmane *et al.* (2019). It can also be noted that the results of Kaci *et al* (2020) obtained by the FSDT method deviate a little bit from the rest of the results.

By introducing the volume fraction of porosity (α), it can be noted that the increase of this factor induces an increase in the results, which shows that the porosity has a significant influence on the free vibration behavior of FG plates.

For the fundamental frequency parameters in the form of $\tilde{\beta} = \omega a^2 \sqrt{\rho_c/E_c}/h$, we can extricate the same remarks. According to Table 4, the results of the present method are in good agreement with those of Tounsi *et al.* (2020).

The results presented in Tables 3 and 4 reveal that the increase in volume fraction porosity (α) increases the fundamental frequency parameters. In order to better visualize the effect of the distribution shape of porosity on the free vibration behavior of FGM plate, it is preferable to present the fundamental frequency parameter defined as $\tilde{\beta} = \omega a^2 \sqrt{\rho_c/E_c}/h$.

The study is applied to FG plate with simply supported boundary conditions, resting on an elastic foundation for deferent aspect ratio a/b (length to width) and thickness ratio h/a (thickness to length), made with Al/ Al₂O₃. The effect of the distribution shape of porosity on the normalized Eigen frequency parameter β is investigated for rectangular FG plates ($a/b=3$) with various values of Pasternak elastic foundations parameters (K_0 and K_1), when the thickness ratio $h/a=0.01, 0.05, 0.1, 0.2$.

In Fig. 2, we present the fundamental frequency parameter $\tilde{\beta}$ of FG rectangular plate ($a/b=3$), resting on an elastic foundation for deferent thickness ratio h/a , under the influence of the distribution shape of porosity when $K_0=K_1=10$.

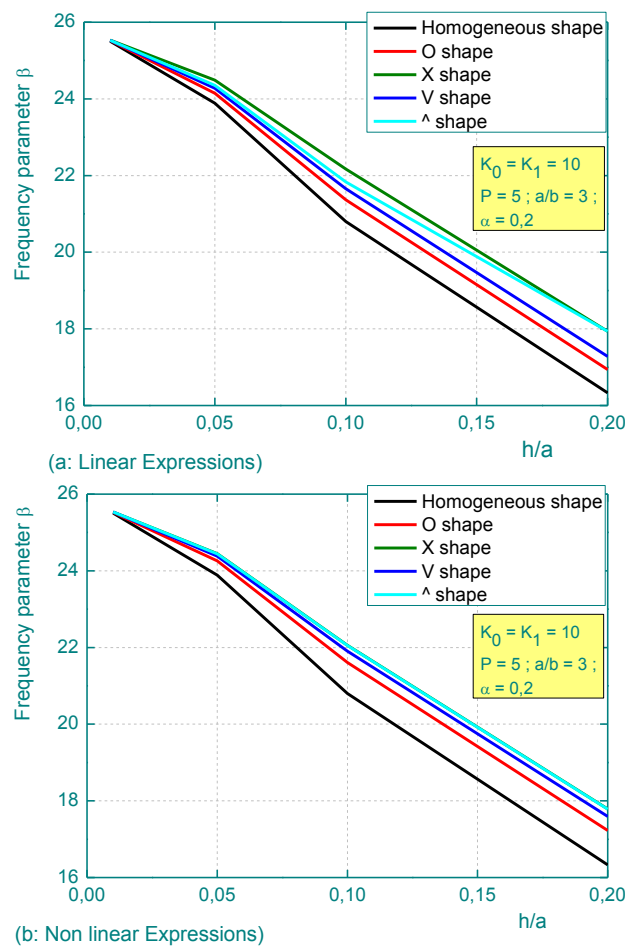


Fig. 2 Effect of the shape of porosity distribution on fundamental frequency parameter $\tilde{\beta}$ versus thickness ratio h/a of an Al/Al₂O₃ FG plate resting on an elastic foundation (a) Linear expressions (b) Nonlinear expressions

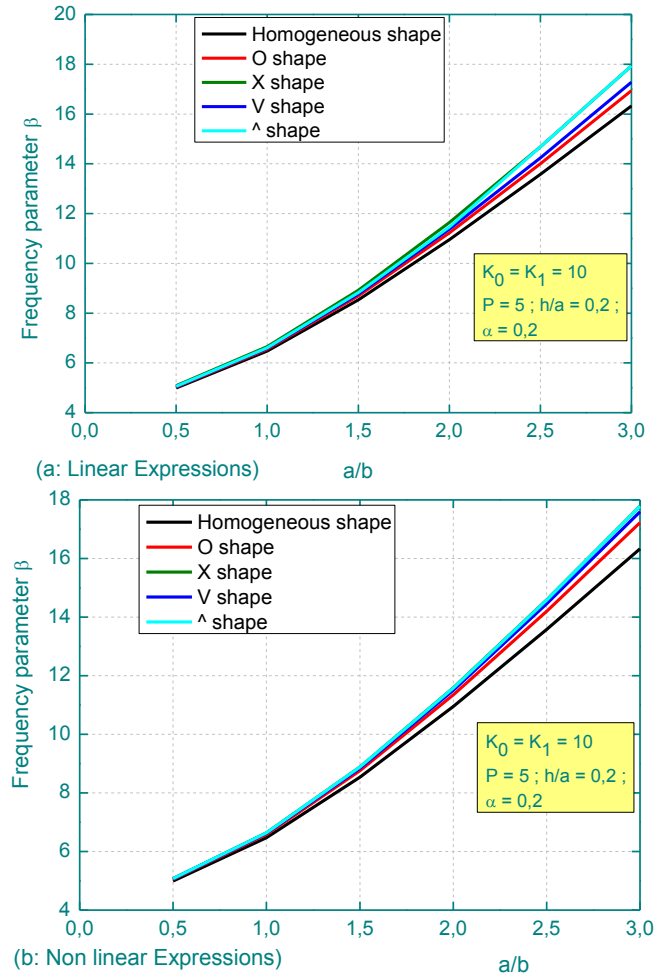


Fig. 3 Effect of the shape of porosity distribution on fundamental frequency parameter $\tilde{\beta}$ versus aspect ratio a/b of an Al/Al_2O_3 FG plate resting on an elastic foundation (a) Linear expressions; (b) Nonlinear expressions

As we can see on Fig. 2, the frequency parameter β decreases as the thickness of the plate increases. The effect of the distribution shape of porosity significantly increases for the thicker plates. In fact, there is no effect for the thin plate ($h/a=0,01$) but the influence occurs when the thickness increases. In the case of linear expressions of the distribution shape of porosity, the curves are clearly separated and distant each other and located above the homogeneous shape's curve (Fig. 2(a)). In the case of nonlinear expressions, the curves are closer to each other and also located above the homogeneous shape's curve (Fig. 2(b)). It can be noted that the distribution shape of porosity has a significant effect on the free vibration of FG plate. Regarding the form of the expressions of the distribution shape of porosity (linear or nonlinear), it seems that there is just a slight influence.

In Fig. 3, we present the fundamental frequency parameter $\tilde{\beta}$ of FG thick plate ($h/a=0.2$), resting on an elastic foundation for deferent aspect ratio a/b , under the influence of the distribution shape of porosity when $K_0=K_1=10$.

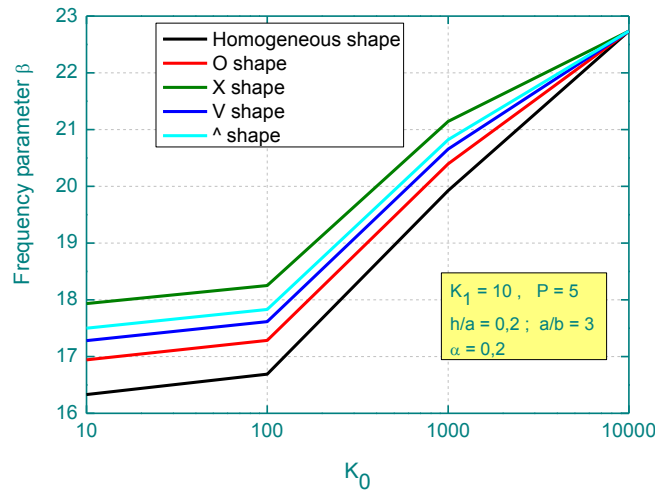


Fig. 4 Effect of the shape of porosity distribution on fundamental frequency parameter $\tilde{\beta}$ versus Pasternak elastic foundations parameter (K_0) of an Al/Al₂O₃ FG plate

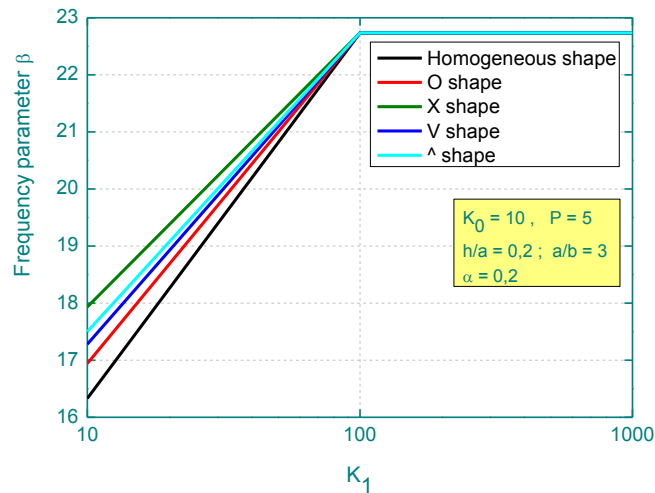


Fig. 5 Effect of the shape of porosity distribution on fundamental frequency parameter $\tilde{\beta}$ versus Pasternak elastic foundations parameter (K_1) of an Al/Al₂O₃ FG plate

As we can see on Fig. 3, the frequency parameter β increases gradually as the width of the plate increases. It can be noted that the effect of the distribution shape of porosity significantly increases for the wider plates. Indeed, the effect appears from a geometric aspect ratio of 1.5 and occurs when the width increases. Practically, we observed the same tendency as for the thickness ratio (h/a).

The form of the expressions of the distribution shape of porosity (linear or nonlinear) has only a slight influence as observed for the thickness ratio effect. This is the reason why, in the following, only linear expressions of the distribution shape of porosity will be considered.

The effect of Pasternak elastic foundations parameters (K_0 and K_1) on the normalized Eigen frequency parameter β is investigated for rectangular FG plates ($a/b=3$) with various distribution shape of porosity, when the thickness ratio $h/a=0.2$, as shown in Fig. 4 and Fig. 5.

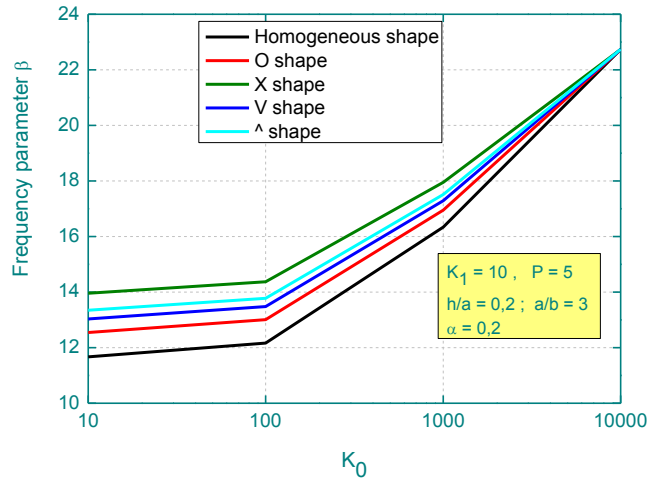


Fig. 6 Effect of the shape of porosity distribution on fundamental frequency parameter β versus Winkler elastic foundation parameter (K_0) of an Al/Al₂O₃ FG plate

By fixing the shear stiffness coefficient of the foundation (K_1) to 10, we can note that the effect of the distribution shape of porosity decreases as the transverse stiffness coefficient increases (Fig. 4). For a high values of transverse stiffness coefficient ($K_0=10000$), there is no effect of the distribution shape of porosity, which means that for a very stiff foundation (in the vertical direction) this effect completely disappears.

In Fig. 5, we present the effect of the distribution shape of porosity on the frequency parameter β versus the shear stiffness coefficient (K_1) for a fixed transverse stiffness coefficient (K_0). It is found that the effect of the distribution shape of porosity only appears for small values of K_1 ($K_1=10$). From $k_1=100$, the effect of distribution shape of porosity completely disappears, which means that the shear stiffness coefficient has only a significant effect when it takes a small values.

For the particular case of Winkler elastic foundation ($K_1=0$), it can be noted a similar tendency that observed for the Pasternak elastic foundation (Fig. 6). However, the effect of the distribution shape of porosity decreases by increasing the Winkler elastic foundation parameter and completely disappears for a high values of this factor ($K_0=10000$).

4. Conclusions

In the present study, the effect of the distribution shape of porosity on the normalized Eigen frequency parameter was investigated for rectangular FG plates resting on Winkler-Pasternak elastic foundations. A parametric study was conducted, including geometric aspect ratios (a/b), thickness ratios (h/a) and foundation stiffness parameters. It was found that the effect of the distribution shape of porosity significantly occurs when the thickness of the plate increases and the length to width ratio (a/b) increases. It was also found that the effect appears for small values of elastic foundations parameters. It can be concluded that the distribution shape of porosity has a significant effect on the free vibration behavior of thick rectangular FG plates for a small values of Winkler-Pasternak elastic foundation parameters.

Acknowledgments

This research was supported by the Algerian Ministry of Higher Education and Scientific Research (MESRS) as part of the grant for the PRFU research project n° A01L02UN140120200002 and by the University of Tiaret, in Algeria.

References

- Abdederak, R., Hassaine Daouadji, T., Benferhat, R. and Adim, B. (2018), "Nonlinear analysis of damaged RC beams strengthened with glass fiber reinforced polymer plate under symmetric loads", *Earthq. Struct.*, **15**(2), 113-122. <https://doi.org/10.12989/eas.2018.15.2.113>.
- Abdelhak, Z., Hadji, L., Khelifa, Z., Hassaine Daouadji, T. and Adda Bedia, E.A. (2016), "Analysis of buckling response of functionally graded sandwich plates using a refined shear deformation theory", *Wind Struct.*, **22**(3), 291-305. <https://doi.org/10.12989/was.2016.22.3.291>.
- Abdelhak, Z., Hadji, L., Khelifa, Z., Hassaine Daouadji, T. and Adda Bedia, E.A. (2016), "Analysis of buckling response of functionally graded sandwich plates using a refined shear deformation theory", *Wind Struct.*, **22**(3), 291-305. <https://doi.org/10.12989/was.2016.22.3.291>.
- Abderezak, R., Daouadji, T.H. and Rabia, B. (2020), "Analysis of interfacial stresses of the reinforced concrete foundation beams repairing with composite materials plate", *Coupl. Syst. Mech.*, **9**(5), 473-498. <http://dx.doi.org/10.12989/csm.2020.9.5.473>.
- Ait Atmane, H., Mokhtar, N., Bennai, R., Tounsi, A. and Adda Bedia, E.A. (2019), "Vibration response and wave propagation in FG plates resting on elastic foundations using HSDT", *Struct. Eng. Mech.*, **69**(5), 511-525. <https://doi.org/10.12989/sem.2019.69.5.511>.
- Al-Furjan, M.S.H., Habibi, M., Chen, G., Safarpour, H., Safarpour, M. and Tounsi, A. (2020b), "Chaotic simulation of the multi-phase reinforced thermo-elastic disk using GDQM", *Eng. Comput.*, 1-24. <https://doi.org/10.1007/s00366-020-01144-2>.
- Al-Furjan, M.S.H., Habibi, M., Ni, J., won Jung, D. and Tounsi, A. (2020), "Frequency simulation of viscoelastic multi-phase reinforced fully symmetric systems", *Eng. Comput.*, 1-17. <https://doi.org/10.1007/s00366-020-01200-x>.
- Al-Furjan, M.S.H., Habibi, M., won Jung, D., Sadeghi, S., Safarpour, H., Tounsi, A. and Chen, G. (2020d), "A computational framework for propagated waves in a sandwich doubly curved nanocomposite panel", *Eng. Comput.*, 1-18. <https://doi.org/10.1007/s00366-020-01130-8>.
- Al-Furjan, M.S.H., hatami, A., Habibi, M., Shan, L. and Tounsi, A. (2021), "On the vibrations of the imperfect sandwich higher-order disk with a lactic core using generalize differential quadrature method", *Compos. Struct.*, 113150. <https://doi.org/10.1016/j.compstruct.2020.113150>.
- Al-Furjan, M.S.H., Safarpour, H., Habibi, M., Safarpour, M. and Tounsi, A. (2020c), "A comprehensive computational approach for nonlinear thermal instability of the electrically FG-GPLRC disk based on GDQ method", *Eng. Comput.*, 1-18. <https://doi.org/10.1007/s00366-020-01088-7>.
- Alimirzaei, S., Mohammadimehr, M. and Tounsi, A. (2019), "Nonlinear analysis of viscoelastic micro-composite beam with geometrical imperfection using FEM: MSGT electro-magneto-elastic bending, buckling and vibration solutions", *Struct. Eng. Mech.*, **71**(5), 485-502. <https://doi.org/10.12989/sem.2019.71.5.485>.
- Balubaid, M., Tounsi, A., Dakhel, B. and Mahmoud, S.R. (2019), "Free vibration investigation of FG nanoscale plate using nonlocal two variables integral refined plate theory", *Comput. Concrete*, **24**(6), 579-586. <https://doi.org/10.12989/cac.2019.24.6.579>.
- Batou, B., Nebab, M., Bennai, R., Atmane, H.A., Tounsi, A. and Bouremana, M. (2019), "Wave dispersion properties in imperfect sigmoid plates using various HSDTs", *Steel Compos. Struct.*, **33**(5), 699-716. <https://doi.org/10.12989/scs.2019.33.5.699>.
- Belbachir, N., Bourada, M., Draiche, K., Tounsi, A., Bourada, F., Bousahla, A.A. and Mahmoud, S.R. (2020),

- “Thermal flexural analysis of anti-symmetric cross-ply laminated plates using a four variable refined theory” *Smart Struct. Syst.*, **25**(4), 409-422. <http://dx.doi.org/10.12989/sss.2020.25.4.409>.
- Belbachir, N., Draich, K., Bousahla, A.A., Bourada, M., Tounsi, A. and Mohammadimehr, M. (2019), “Bending analysis of anti-symmetric cross-ply laminated plates under nonlinear thermal and mechanical loadings”, *Steel Compos. Struct.*, **33**(1), 81-92. <https://doi.org/10.12989/scs.2019.33.1.081>.
- Belkacem, A. and Hassaine Daouadji, T. (2016), “Effects of thickness stretching in FGM plates using a quasi-3D higher order shear deformation theory”, *Adv. Mater. Res.*, **5**(4), 223-244. <https://doi.org/10.12989/amr.2016.5.4.223>.
- Belkacem, A., Tahar, H.D., Abderrezak, R., Amine, B.M., Mohamed, Z. and Boussad, A. (2018), “Mechanical buckling analysis of hybrid laminated composite plates under different boundary conditions”, *Struct. Eng. Mech.*, **66**(6), 761-769. <https://doi.org/10.12989/sem.2018.66.6.761>.
- Bellal, M., Hebali, H., Heireche, H., Bousahla, A.A., Tounsi, A., Bourada, F., ... & Tounsi, A. (2020), “Buckling behavior of a single-layered graphene sheet resting on viscoelastic medium via nonlocal four-unknown integral model”, *Steel Compos. Struct.*, **34**(5), 643-655. <https://doi.org/10.12989/scs.2020.34.5.643>.
- Benferhat, R., Daouadji, T.H., Mansour, M.S. and Hadji, L. (2016), “Effect of porosity on the bending and free vibration response of functionally graded plates resting on Winkler-Pasternak foundations”, *Earthq. Struct.*, **10**(5), 1429-1449. <https://doi.org/10.12989/eas.2016.10.5.1033>.
- Benferhat, R., Hassaine Daouadji, T., Hadji, L. and Said Mansour, M. (2016), “Static analysis of the FGM plate with porosities”, *Steel Compos. Struct.*, **21**(1), 123-136. <https://doi.org/10.12989/scs.2016.21.1.123>.
- Benhenni, M.A., Adim, B., Daouadji, T.H., Abbès, B., Abbès, F., Li, Y. and Bouzidane, A. (2019), “A comparison of closed form and finite element solutions for the free vibration of hybrid cross ply laminated plates”, *Mech. Compos. Mater.*, **55**(2), 181-194. <https://doi.org/10.1007/s11029-019-09803-2>.
- Benhenni, M.A., Daouadji, T.H., Abbes, B., Abbes, F., Li, Y. and Adim, B. (2019), “Numerical analysis for free vibration of hybrid laminated composite plates for different boundary conditions”, *Struct. Eng. Mech.*, **70**(5), 535-549. <https://doi.org/10.12989/sem.2019.70.5.535>.
- Benhenni, M.A., Daouadji, T.H., Abbes, B., Adim, B., Li, Y. and Abbes, F. (2018), “Dynamic analysis for anti-symmetric cross-ply and angle-ply laminates for simply supported thick hybrid rectangular plates”, *Adv. Mater. Res.*, **7**(2), 83-103. <https://doi.org/10.12989/amr.2018.7.2.119>.
- Bensattalah, T., Daouadji, T.H., Zidour, M., Tounsi, A. and Bedia, E.A. (2016), “Investigation of thermal and chirality effects on vibration of single walled carbon nanotubes embedded in a polymeric matrix using nonlocal elasticity theories”, *Mech. Compos. Mater.*, **52**(4), 555-568. <https://doi.org/10.1007/s11029-016-9606-z>.
- Bensattalah, T., Zidour, M. and Daouadji, T.H. (2018), “Analytical analysis for the forced vibration of CNT surrounding elastic medium including thermal effect using nonlocal Euler-Bernoulli theory”, *Adv. Mater. Res.*, **7**(3), 163-174. <https://doi.org/10.12989/amr.2018.7.3.163>.
- Berghouti, H., Adda Bedia, E.A., Benkhedda, A. and Tounsi, A. (2019), “Vibration analysis of nonlocal porous nanobeams made of functionally graded material”, *Adv. Nano Res.*, **7**(5), 351-364. <https://doi.org/10.12989/anr.2019.7.5.351>.
- Bouakaz, K., Daouadji, T.H., Meftah, S.A., Ameer, M., Tounsi, A. and Bedia, E.A. (2014), “A numerical analysis of steel beams strengthened with composite materials”, *Mech. Compos. Mater.*, **50**(4), 685-696. <https://doi.org/10.1007/s11029-014-9435-x>.
- Boulefrakh, L., Hebali, H., Chikh, A., Bousahla, A.A., Tounsi, A. and Mahmoud, S.R. (2019), “The effect of parameters of visco-Pasternak foundation on the bending and vibration properties of a thick FG plate”, *Geomech. Eng.*, **18**(2), 161-178. <https://doi.org/10.12989/gae.2019.18.2.161>.
- Bourada, F., Bousahla, A.A., Tounsi, A., Bedia, E.A., Mahmoud, S.R., Benrahou, K.H. and Tounsi, A. (2020), “Stability and dynamic analyses of SW-CNT reinforced concrete beam resting on elastic-foundation”, *Comput. Concrete*, **25**(6), 485-495. <https://doi.org/10.12989/cac.2020.25.6.485>.
- Bourada, F., Bousahla, A.A., Tounsi, A., Bedia, E.A., Mahmoud, S.R., Benrahou, K.H. and Tounsi, A. (2020), “Stability and dynamic analyses of SW-CNT reinforced concrete beam resting on elastic-foundation”, *Comput. Concrete*, **25**(6), 485-495. <https://doi.org/10.12989/cac.2020.25.6.485>.

- Boussoula, A., Boucham, B., Bourada, M., Bourada, F., Tounsi, A., Bousahla, A.A. and Tounsi, A. (2020), "A simple nth-order shear deformation theory for thermomechanical bending analysis of different configurations of FG sandwich plates", *Smart Struct. Syst.*, **25**(2), 197-218. <https://doi.org/10.12989/sss.2020.25.2.197>.
- Chaabane, L.A., Bourada, F., Sekkal, M., Zerouati, S., Zaoui, F.Z., Tounsi, A., ... & Tounsi, A. (2019), "Analytical study of bending and free vibration responses of functionally graded beams resting on elastic foundation", *Struct. Eng. Mech.*, **71**(2), 185-196. <https://doi.org/10.12989/sem.2019.71.2.185>.
- Chedad, A., Daouadji, T.H., Abderezak, R., Adim, B., Abbes, B., Rabia, B. and Abbes, F. (2018), "A high-order closed-form solution for interfacial stresses in externally sandwich FGM plated RC beams", *Adv. Mater. Res.*, **6**(4), 317-328. <https://doi.org/10.12989/amr.2017.6.4.317>.
- Chergui, S., Daouadji, T.H., Hamrat, M., Boulekbache, B., Bougara, A., Abbes, B. and Amziane, S. (2019), "Interfacial stresses in damaged RC beams strengthened by externally bonded prestressed GFRP laminate plate: Analytical and numerical study", *Adv. Mater. Res.*, **8**(3), 197-217. <https://doi.org/10.12989/amr.2019.8.3.197>.
- Chikr, S.C., Kaci, A., Bousahla, A.A., Bourada, F., Tounsi, A., Bedia, E.A., ... & Tounsi, A. (2020), "A novel four-unknown integral model for buckling response of FG sandwichplates resting on elastic foundations under various boundary conditions using Galerkin's approach", *Geomech. Eng.*, **21**(5), 471-487. <https://doi.org/10.12989/gae.2020.21.5.471>.
- Daouadji, H.T. (2013), "Analytical analysis of the interfacial stress in damaged reinforced concrete beams strengthened by bonded composite plates", *Strength Mater.*, **45**(5), 587-597. <https://doi.org/10.1007/s11223-013-9496-4>.
- Daouadji, H.T. (2017), "Analytical and numerical modeling of interfacial stresses in beams bonded with a thin plate", *Adv. Comput. Des.*, **2**(1) 57-69. <https://doi.org/10.12989/acd.2017.2.1.057>.
- Daouadji, T. H., & Benferhat, R. (2016), "Bending analysis of an imperfect FGM plates under hygro-thermo-mechanical loading with analytical validation", *Adv. Mater. Res.*, **5**(1), 35-53. <https://doi.org/10.12989/amr.2016.5.1.035>.
- Daouadji, T.H. (2016b), "Theoretical analysis of composite beams under uniformly distributed load", *Adv. Mater. Res.*, **5**(1), 1-9. <https://doi.org/10.12989/amr.2016.5.1.001>.
- Daouadji, T.H. and Adim, B. (2016a), "An analytical approach for buckling of functionally graded plates", *Adv. Mater. Res.*, **5**(3), 141-169. <https://doi.org/10.12989/amr.2016.5.3.141>.
- Daouadji, T.H., Benferhat, R. and Adim, B. (2016), "Bending analysis of an imperfect advanced composite plates resting on the elastic foundations", *Coupl. Syst. Mech.*, **5**(3), 269-285. <http://dx.doi.org/10.12989/csm.2017.5.3.269>.
- Daouadji, T.H., Rabahi, A., Abbes, B. and Adim, B. (2016), "Theoretical and finite element studies of interfacial stresses in reinforced concrete beams strengthened by externally FRP laminates plate", *J. Adhes. Sci. Technol.*, **30**(12), 1253-1280. <https://doi.org/10.1080/01694243.2016.1140703>.
- Draiche, K., Bousahla, A.A., Tounsi, A., Alwabli, A.S., Tounsi, A. and Mahmoud, S.R. (2019), "Static analysis of laminated reinforced composite plates using a simple first-order shear deformation theory", *Comput. Concrete*, **24**(4), 369-378. <https://doi.org/10.12989/cac.2019.24.4.369>.
- Hadj, B., Rabia, B. and Daouadji, T.H. (2019), "Influence of the distribution shape of porosity on the bending FGM new plate model resting on elastic foundations", *Struct. Eng. Mech.*, **72**(1), 823-832. <https://doi.org/10.12989/sem.2019.72.1.061>.
- Hamrat, M., Bouziadi, F., Boulekbache, B., Daouadji, T.H., Chergui, S., Labed, A. and Amziane, S. (2020), "Experimental and numerical investigation on the deflection behavior of pre-cracked and repaired reinforced concrete beams with fiber-reinforced polymer", *Constr. Build. Mater.*, **249**(20), 1-13. <https://doi.org/10.1016/j.conbuildmat.2020.118745>.
- Hosseini-Hashemi, S., Fadaee, M. and Atashipour, S.R. (2011), "Study on the free vibration of thick functionally graded rectangular plates according to a new exact closed-form procedure", *Compos. Struct.*, **93**(2), 722-735. <https://doi.org/10.1016/j.compstruct.2010.08.007>.
- Hussain, M., Naem, M.N., Khan, M.S. and Tounsi, A. (2020), "Computer-aided approach for modelling of FG cylindrical shell sandwich with ring supports", *Comput. Concrete*, **25**(5), 411-425.

- <https://doi.org/10.12989/cac.2020.25.5.411>.
- Kaddari, M., Kaci, A., Bousahla, A.A., Tounsi, A., Bourada, F., Tounsi, A., ... & Al-Osta, M.A. (2020), "A study on the structural behaviour of functionally graded porous plates on elastic foundation using a new quasi-3D model: Bending and Free vibration analysis", *Comput. Concrete*, **25**(1), 37-57. <https://doi.org/10.12989/cac.2020.25.1.037>.
- Khadimallah, M.A., Hussain, M., Khedher, K.M., Naeem, M.N. and Tounsi, A. (2020), "Backward and forward rotating of FG ring support cylindrical shells", *Steel Compos. Struct.*, **37**(2), 137-150. <http://dx.doi.org/10.12989/scs.2020.37.2.137>.
- Khiloun, M., Bousahla, A.A., Kaci, A., Bessaim, A., Tounsi, A. and Mahmoud, S.R. (2020), "Analytical modeling of bending and vibration of thick advanced composite plates using a four-variable quasi 3D HSDT", *Eng. Comput.*, **36**(3), 807-821. <https://doi.org/10.1007/s00366-019-00732-1>.
- Mahmoudi, A., Benyoucef, S., Tounsi, A., Benachour, A., Adda Bedia, E.A. and Mahmoud, S.R. (2019), "A refined quasi-3D shear deformation theory for thermo-mechanical behavior of functionally graded sandwich plates on elastic foundations", *J. Sandw. Struct. Mater.*, **21**(6), 1906-1926. <https://doi.org/10.1177/1099636217727577>.
- Matouk, H., Bousahla, A.A., Heireche, H., Bourada, F., Bedia, E.A., Tounsi, A., ... & Benrahou, K.H. (2020), "Investigation on hygro-thermal vibration of P-FG and symmetric S-FG nanobeam using integral Timoshenko beam theory", *Adv. Nano Res.*, **8**(4), 293-305. <https://doi.org/10.12989/anr.2020.8.4.293>.
- Matsunaga, H. (2008), "Free vibration and stability of functionally graded plates according to a 2-D higher-order deformation theory", *Compos. Struct.*, **82**(4), 499-512. <http://dx.doi.org/10.1016/j.compstruct.2007.01.030>.
- Praveen, G.N. and Reddy, J.N. (1998), "Nonlinear transient thermoelastic analysis of functionally graded ceramic-metal plates", *Int. J. Solid. Struct.*, **35**(33), 4457-4476. [https://doi.org/10.1016/S0020-7683\(97\)00253-9](https://doi.org/10.1016/S0020-7683(97)00253-9).
- Rabahi, A., Benferhat, R. and Daouadji, H.T. (2019), "Elastic analysis of interfacial stresses in prestressed PFGM-RC hybrid beams", *Adv. Mater. Res.*, **7**(2), 83-103. <https://doi.org/10.12989/amr.2018.7.2.083>.
- Rabahi, A., Daouadji, T.H., Abbes, B. and Adim, B. (2016), "Analytical and numerical solution of the interfacial stress in reinforced-concrete beams reinforced with bonded prestressed composite plate", *J. Reinf. Plast. Compos.*, **35**(3) 258-272. <https://doi.org/10.1177/0731684415613633>.
- Rabhi, M., Benrahou, K.H., Kaci, A., Houari, M.S.A., Bourada, F., Bousahla, A.A., ... & Tounsi, A. (2020), "A new innovative 3-unknowns HSDT for buckling and free vibration of exponentially graded sandwich plates resting on elastic foundations under various boundary conditions", *Geomech. Eng.*, **22**(2), 119-132. <https://doi.org/10.12989/gae.2020.22.2.119>.
- Rabia, B., Abderezak, R., Daouadji, T.H., Abbes, B., Belkacem, A. and Abbes, F. (2018), "Analytical analysis of the interfacial shear stress in RC beams strengthened with prestressed exponentially-varying properties plate", *Adv. Mater. Res.*, **7**(1), 29-44. <https://doi.org/10.12989/amr.2018.7.1.029>.
- Rabia, B., Daouadji, T.H. and Abderezak, R. (2019), "Effect of distribution shape of the porosity on the interfacial stresses of the FGM beam strengthened with FRP plate", *Earthq. Struct.*, **16**(5), 601-609. <https://doi.org/10.12989/eas.2019.16.5.601>.
- Rahmani, M.C., Kaci, A., Bousahla, A.A., Bourada, F., Tounsi, A., Bedia, E.A., ... & Tounsi, A. (2020), "Influence of boundary conditions on the bending and free vibration behavior of FGM sandwich plates using a four-unknown refined integral plate theory", *Comput. Concrete*, **25**(3), 225-244. <https://doi.org/10.12989/cac.2020.25.3.225>.
- Refrafi, S., Bousahla, A.A., Bouhadra, A., Menasria, A., Bourada, F., Tounsi, A., Adda Bedia, E.A., Mahmoud, S.R., Benrahou, K.H. and Tounsi, A. (2020), "Effects of hygro-thermo-mechanical conditions on the buckling of FG sandwich plates resting on elastic foundations", *Comput. Concrete*, **25**(4), 311-325. <https://doi.org/10.12989/cac.2020.25.4.311>.
- Tahar, H.D., Abderezak, R. and Rabia, B. (2020), "Flexural performance of wooden beams strengthened by composite plate", *Struct. Monit. Mainten.*, **7**(3), 233-259. <http://dx.doi.org/10.12989/smm.2020.7.3.233>.
- Tahar, H.D., Boussad, A., Abderezak, R., Rabia, B., Fazilay, A. and Belkacem, A. (2019), "Flexural behaviour of steel beams reinforced by carbon fibre reinforced polymer: Experimental and numerical study", *Struct.*

- Eng. Mech.*, **72**(4), 409-419. <https://doi.org/10.12989/sem.2019.72.4.409>.
- Tayeb, B. and Daouadji, T.J. (2020), "Improved analytical solution for slip and interfacial stress in composite steel-concrete beam bonded with an adhesive", *Adv. Mater. Res.*, **9**(2), 133-153. <https://doi.org/10.12989/amr.2020.9.2.133>.
- Thai, H.T. and Kim, S.E. (2013), "Closed-form solution for buckling analysis of thick functionally graded plates on elastic foundation", *Int. J. Mech. Sci.*, **75**, 34-44. <http://dx.doi.org/10.1016/j.ijmecsci.2013.06.007>.
- Tounsi, A., Al-Dulaijan, S.U., Al-Osta, M.A., Chikh, A., Al-Zahrani, M.M., Sharif, A. and Tounsi, A. (2020), "A four variable trigonometric integral plate theory for hygro-thermo-mechanical bending analysis of AFG ceramic-metal plates resting on a two-parameter elastic foundation", *Steel Compos. Struct.*, **34**(4), 511-524. <https://doi.org/10.12989/scs.2020.34.4.511>.
- Tounsi, A., Daouadji, T.H. and Benyoucef, S. (2008), "Interfacial stresses in FRP-plated RC beams: Effect of adherend shear deformations", *Int. J. Adhes. Adhesiv.*, **29**, 313-351. <https://doi.org/10.1016/j.ijadhadh.2008.06.008>.
- Wattanasakulponga, N. and Ungbhakornb, V. (2014), "Linear and nonlinear vibration analysis of elastically restrained ends FGM beams with porosities", *Aerosp. Sci. Technol.*, **32**(1), 111-120. <https://doi.org/10.1016/j.ast.2013.12.002>.
- Zhao, X., Lee, Y.Y. and Liew, K.M. (2009), "Free vibration analysis of functionally graded plates using the element-free kp-Ritz method", *J. Sound Vib.*, **319**, 918-939. <https://doi.org/10.1016/j.jsv.2008.06.025>.
- Zine, A., Bousahla, A.A., Bourada, F., Benrahou, K.H., Tounsi, A., Adda Bedia, E.A., ... & Tounsi, A. (2020), "Bending analysis of functionally graded porous plates via a refined shear deformation theory", *Comput. Concrete*, **26**(1), 63-74. <http://dx.doi.org/10.12989/cac.2020.26.1.063>.